André Zabel | Alette Winter | Alexandra Kelling | Uwe Schilde
Peter Strauch

Tetrabromidocuprates(II)—Synthesis, Structure and EPR

Suggested citation referring to the original publication:
Int. J. Mol. Sci. 17 (2016)
DOI http://dx.doi.org/10.3390/ijms17040596

International Journal of
Molecular Sciences

MDPI

Article

Tetrabromidocuprates(II)—Synthesis, Structure and EPR

André Zabel [1], Alette Winter [2], Alexandra Kelling [1], Uwe Schilde [1] and Peter Strauch [1,*]

[1] Institute of Chemistry, University of Potsdam, Karl-Liebknechtstr.-Str. 24-25, Potsdam D-14476, Germany; azabel@uni-potsdam.de (A.Z.); kelling@uni-potsdam.de (A.K.); uschilde@uni-potsdam.de (U.S.)

[2] Engineering Education Research Group, Hamburg University of Technology (TUHH), Am Schwarzberg-Campus 3 (E), Hamburg D-21073, Germany; alette.winter@tuhh.de

* Correspondence: pstrauch@uni-potsdam.de; Tel.: +49-331-977-5268

Academic Editors: Peter Hesemann and Andreas Taubert
Received: 16 March 2016; Accepted: 14 April 2016; Published: 20 April 2016

Abstract: Metal-containing ionic liquids (ILs) are of interest for a variety of technical applications, e.g., particle synthesis and materials with magnetic or thermochromic properties. In this paper we report the synthesis of, and two structures for, some new tetrabromidocuprates(II) with several "onium" cations in comparison to the results of electron paramagnetic resonance (EPR) spectroscopic analyses. The sterically demanding cations were used to separate the paramagnetic Cu(II) ions for EPR measurements. The EPR hyperfine structure in the spectra of these new compounds is not resolved, due to the line broadening resulting from magnetic exchange between the still-incomplete separated paramagnetic Cu(II) centres. For the majority of compounds, the principal g values ($g_{||}$ and $g_{\perp}$) of the tensors could be determined and information on the structural changes in the $[CuBr_4]^{2-}$ anions can be obtained. The complexes have high potential, e.g., as ionic liquids, as precursors for the synthesis of copper bromide particles, as catalytically active or paramagnetic ionic liquids.

Keywords: tetrabromidocuprate(II); X-ray structure; electron paramagnetic resonance; copper(II)

1. Introduction

Metal-containing ionic liquids (ILs) or ionic liquid crystals (ILCs) are of interest for a variety of technical applications, e.g., as precursors for the synthesis of (nano)particles, magnetic or thermochromic materials [1–3] or as extraction agents [4] and catalysts [5–8]. Tetrahalidometalate complexes exhibit many of these interesting properties. Also liquid-crystalline ILs based on tetrahalidometalates have been reported [9–13]. Some ILs and ILCs combining tetrahalidocuprate dianions with alkylpyridinium cations can serve as precursors for inorganic materials [2,14–17]. A variety of these metal-containing ionic liquids show interesting electrochemical properties as electrochromy and/or magnetic behaviour [18,19]. The properties of ionic liquid materials such as tuneable acidity, polarity, amphiphilic character, coordinating ability, and miscibility with many compounds might be combined with the unique properties introduced by the metal ions. ILs of this type are also of interest as catalysts, as alternative solvents and even morphology templates for inorganic materials simultaneously. Reports on tetrahalidometalate-based ILs/ILCs and their applications as well as their structural characterization are still relatively rare [2,10–13,20–32]. We present the syntheses, electron paramagnetic resonance (EPR) spectra and two X-ray structures of some new tetrabromidocuprate(II) compounds. The following cations with different steric demand were used to separate the paramagnetic Cu(II) ions for the EPR measurements (see Scheme 1): the homogenously substituted tetraalkyl onium cations with varying chain lengths tetraethylammonium, (Et_4N^+), tetrabutylphosphonium, (Bu_4P^+), tetrahexylammonium, (Hex_4N^+), the benzyl/alkyl substituted ammonium cations benzyltrimethylammonium, ($BzlMe_3N^+$), benzyltriethylammonium,

($BzlEt_3N^+$), benzyltributylammonium, ($BzlBu_3N^+$), the alkyltriphenylphosphonium cations ethyltriphenylphosphonium, ($EtPh_3P^+$), hexyltriphenylphosphonium, ($HexPh_3P^+$) and the long chain cations dodecyltrimethylammonium, ($C_{12}H_{25}Me_3N^+$), hexadecylpyridinium, ($C_{16}H_{33}$-py^+), hexadecyldimethylammonium, ($(C_{16}H_{33})_2Me_2N^+$), giving raise to lamellar structures [33]. It is known that tetrahalidocuprate(II)-ions present a high structural flexibility. Thus, the complex anion adopts coordination geometries between square-planar and tetrahedral. Recently we have shown that there is a correlation of EPR parameters and the isotropic or averaged *g*-values with the degree of geometrical distortion in the coordination sphere of tetrahalidocuprates expressed by the *cis*-angle, the average of the four smallest X-Cu-X angles of the tetrahalidocuprate dianion [33–35].

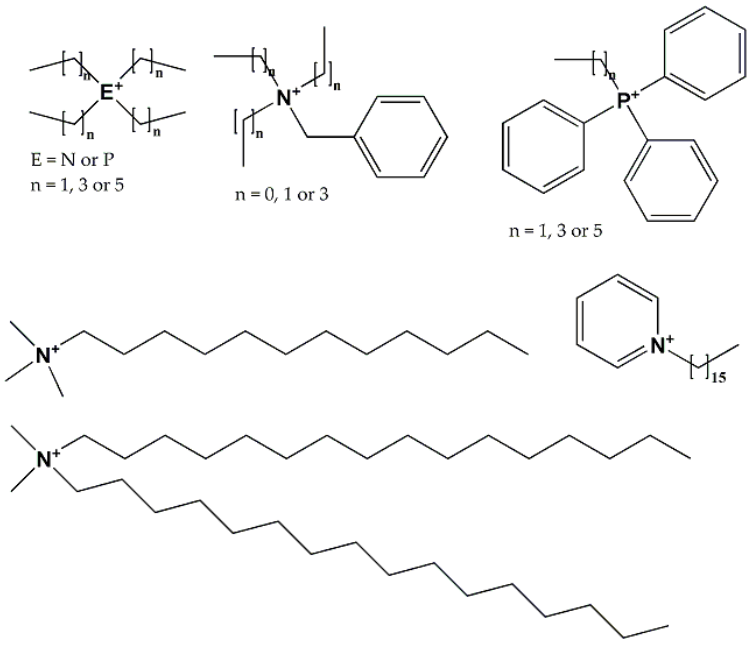

Scheme 1. Cations of the $[CuBr_4]^{2-}$ salts.

2. Results and Discussion

2.1. X-ray Crystallography

Table 1 summarizes the crystallographic data and refinement parameters for the structures of $(BzlEt_3N)_2[CuBr_4]$ (**5**) and $(HexPh_3P)_2[CuBr_4]$ (**8**).

Table 1. Crystallographic data and refinement parameters for (**5**) and (**8**).

Compound	$(BzlEt_3N)_2[CuBr_4]$ (5)	$(HexPh_3P)_2[CuBr_4]$ (8)
Empirical formula	$C_{26}H_{44}N_2CuBr_4$	$C_{48}H_{56}P_2CuBr_4$
M_W/g·mol^{-1}	767.81	1078.04
Crystal description	purple plate	purple needle
Crystal size/mm	0.7 × 0.5 × 0.1	0.8 × 0.2 × 0.1
Crystal system	monoclinic	monoclinic
Space group	$P2_1/c$	$P2_1/n$
a/Å	15.1019(5)	10.7410(3)
b/Å	11.6664(5)	22.4775(9)
c/Å	17.5517(6)	19.6455(6)
α/°	90	90
β/°	99.166(3)	99.807(2)
γ/°	90	90

Table 1. *Cont.*

Compound	$(BzlEt_3N)_2[CuBr_4]$ (5)	$(HexPh_3P)_2[CuBr_4]$ (8)
V/Å^3	3052.9(2)	4673.7(3)
Z	4	4
$F(000)$	1532	2172
Density/mg·m^{-3}	1.67	1.532
μ/mm^{-1}	5.97	3.987
Θ range/°	2.10–25.00	2.15–24.998
R_{int}	0.1338	0.0740
Reflections measured	38,767	73,469
Reflections independent	5372	8223
Parameters	299	496
R_1/wR_2 ($I > 2\sigma(I)$)	0.0370/0.0893	0.0480/0.1183
R_1/wR_2 (all data)	0.0529/0.0975	0.0711/0.1293
Goodness of fit	1.015	1.031
Max. difference peak/hole/e Å^{-3}	0.71/−0.83	2.231/−1.220

2.2. Bis(benzyltriethylammonium)tetrabromidocuprate(II) (5)

$(BzlEt_3N)_2[CuBr_4]$ (**5**) crystallizes in the monoclinic space group $P2_1/c$ with four formula units per unit cell. The corresponding lattice parameters are a = 15.1019(5) Å, b = 11.6664(5) Å, c = 17.5517(6) Å, and β = 99,166(3)°. The complex dianion has a distorted tetrahedral geometry with Br–Cu–Br angles between 98.2° and 131.8° (see Table 2), the resulting *cis*-angle, the average of the four smallest angles, is 99.8°. The shortest Cu···Cu distances are 9.12 and 9.44 Å. Figure 1 shows the molecular structure of $(BzlEt_3N)_2[CuBr_4]$ (**5**). The structure is stabilized by a series of hydrogen bonds (see Table 3).

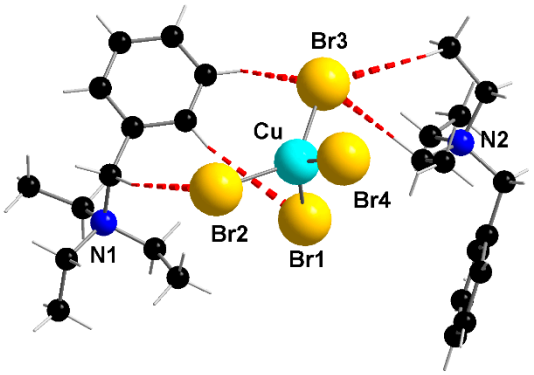

Figure 1. Molecular structure of $(BzlEt_3N)_2[CuBr_4]$ (**5**), hydrogen contacts are presented as fragmented lines.

Table 2. Selected bond lengths and bond angles of $(BzlEt_3N)_2[CuBr_4]$ (**5**).

Bond Lengths/Å		Bond Angles/°	
Cu1–Br1	2.3981(7)	Br1–Cu1–Br2	99.73(2)
		Br1–Cu1–Br3	98.38(2)
		Br1–Cu1–Br4	130.80(3)
Cu1–Br2	2.3747(7)	Br2–Cu1–Br3	131.84(3)
Cu1–Br3	2.3918(7)	Br2–Cu1–Br4	98.19(2)
Cu1–Br4	2.3984(7)	Br3–Cu1–Br4	102.80(2)

Table 3. Hydrogen contacts for $(BzlEt_3N)_2[CuBr_4]$ (**5**).

C–H···Br	H···Br/Å	C···Br/Å	Angles C–H···Br/°
C1–H1A···Br2 [i]	2.93	3.568(4)	124.2
C2–H2A···Br2	3.09	3.955(6)	151.1
C6–H6A···Br2 [ii]	2.82	3.742(6)	161.1
C6–H6A···Br1 [ii]	3.01	3.621(6)	132.2
C7–H7A···Br2 [ii]	2.99	3.935(4)	164.6
C7–H7B···Br3	3.04	3.982(5)	165.4
C14–H14*A*···Br1 [iii]	3.08	3.564(4)	112.3
C14–H14B···Br3	2.92	3.720(5)	140.3
C16–H16A···Br4	3.02	3.849(5)	144.6
C16–H16B···Br1	2.96	3.868(5)	156.9
C20–H20A···Br1 [ii]	3.08	3.982(4)	154.6

Symmetry codes: (i) 1 − x, 2 − y, 1 − z; (ii) 1 − x, 0.5 + y, 0.5 − z; (iii) −x, −0.5 + y, 0.5 − z.

2.3. Bis(hexyltriphenylphosphonium)tetrabromidocuprate(II) (8)

$(HexPh_3P)_2[CuBr_4]$ (**8**) crystallizes in the monoclinic space group $P2_1/n$ with $Z = 4$. The corresponding lattice parameters are a = 10.7410(3) Å, b = 22.4775(9) Å, c = 19.6455(6) Å, and β = 99,807(2)°. This complex dianion has also a distorted tetrahedral geometry with Br–Cu–Br angles between 100.4° and 124.8° (Table 4), with a resulting *cis*-angle of 103.3°. The shortest Cu···Cu distances are 10.62 and 10.74 Å. Figure 2 shows the molecular structure of $(HexPh_3P)_2[CuBr_4]$ (**8**). The structure is stabilized by a variety of hydrogen contacts (Table 5).

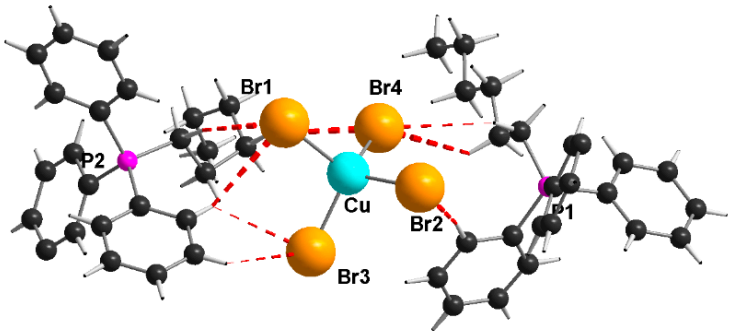

Figure 2. Molecular structure of $(HexPh_3P)_2[CuBr_4]$ (**8**), hydrogen contacts are presented as fragmented lines.

Table 4. Selected bond lengths and bond angles for $(HexPh_3P)_2[CuBr_4]$ (**8**).

Bond Lengths/Å		Bond Angles/°	
		Br1–Cu1–Br2	120.66(4)
Cu1–Br1	2.4500(9)	Br1–Cu1–Br3	103.25(3)
		Br1–Cu1–Br4	104.45(3)
Cu1–Br2	2.3867(9)	Br2–Cu1–Br3	104.95(3)
Cu1–Br3	2.4207(9)	Br2–Cu1–Br4	100.39(3)
Cu1–Br4	2.3677(9)	Br3–Cu1–Br4	124.76(4)

Table 5. Hydrogen bond geometry for $(HexPh_3P)_2[CuBr_4]$ (**8**).

C–H···Br	H···Br/Å	C···Br/Å	Angles C–H···Br/°
C12–H12···Br2	2.82	3.744(6)	166.4
C19–H19B···Br3 [iii]	3.10	4.064(5)	166.4
C26–H26···Br1	3.13	3.840(5)	133.8
C26–H26···Br3	3.07	3.718(6)	127.2
C32–H32···Br4 [ii]	2.90	3.673(5)	140.8
C36–H36···Br2 [i]	2.84	3.776(5)	176.7
C43–H43B···Br1	2.88	3.834(5)	165.9
C43–H43A···Br2 [i]	3.06	4.000(6)	161.1

Symmetry codes: (i) 0,5 + x, 0.5 − y, 0.5 + z; (ii) 1 + x, y, z; (iii) 1 − x, y, z.

2.4. Electron Paramagnetic Resonance (EPR) Spectroscopy

Figure 3 shows a spectrum of $(EtPh_3P)_2[CuBr_4]$ (**7**) at 150 K, characteristic for most of the recorded spectra. In general the spectra are of poor resolution, due to the magnetic interactions between the paramagnetic centers and no hyperfine structure can be observed. Some of the spectra are of axial symmetry and $g_{||}$ as well as $g_{\perp}$ can be determined; for a few samples only an isotropic signal (g_{iso}) could be extracted. The EPR data are shown in Table 6. The g_{av}-values correspond to the isotropic g_{iso}-value of liquid systems as long as strong solvents are excluded (e.g., solutions or ionic liquids).

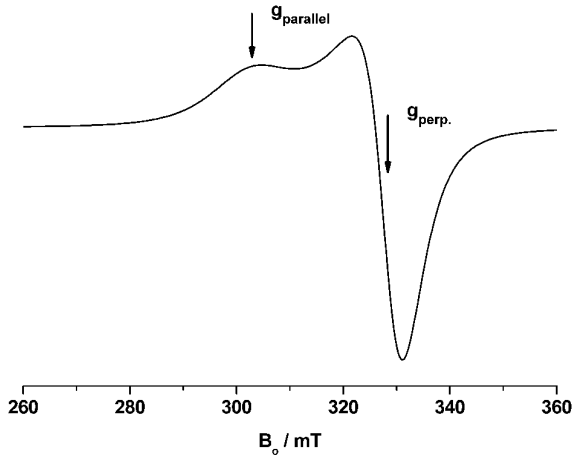

Figure 3. Electron paramagnetic resonance (EPR) spectrum of $(EtPh_3P)_2[CuBr_4]$ (**7**) at 150 K.

Table 6. Experimental g-values ($g_{||}$, $g_{\perp}$ and g_{iso}), calculated values g_{av} and known *cis*-angles (ϕ_{av}) for this series of tetrabromidocuprates(II).

Cation/Compound	$g_{\|\|}$	$g_{\perp}$	g_{iso}	g_{av}	ϕ_{av}/°	Reference (ϕ_{av})
Et_4N^+/(**1**)	-	-	2.18 [a]	-	108.06 *	[36]
Bu_4P^+/(**2**)	-	-	2.089	-	-	
Hex_4P^+/(**3**)	2.34 [a]	2.079	2.11 [a]	2.166	-	
$BzlMe_3N^+$/(**4**)	2.221	2.058	2.101	2.109	99.64 *	[37]
$BzlEt_3N^+$/(**5**)	-	-	2.11 [a]	-	99.77 *	
$BzlBu_3P^+$/(**6**)	-	-	2.108	-	-	
$EtPh_3P^+$/(**7**)	2.217	2.062	-	2.114	-	
$BuPh_3P^+$/(**8**)	2.280	2.069	-	2.139	-	
$HexPh_3P^+$/(**9**)	-	-	2.13 [a]	-	103.26 *	
$(C_{12}H_{25})Me_3N^+$/(**10**)		2.26 [a], 2.124, 2.040		2.141	-	
$(C_{16}H_{33})py^+$/(**11**)	-	-	2.15 [a]	-	-	
$(C_{16}H_{33})_2Me_2N^+$/(**12**)	2.28 [a]	2.079	-	2.146	-	

Experimental errors: g-values: ±0.005; [a] g: ±0.01; *: new added EPR/structure data sets.

The averaged g-values g_{av} for axial symmetry are calculated by the following expression:

$$g_{av} = \frac{g_{II} + 2 \times g_{\perp}}{3} \quad (1)$$

For rhombic symmetry the averaged g-values g_{av} are calculated as follows:

$$g_{av} = \frac{g_1 + g_2 + g_3}{3} \quad (2)$$

The variation of the structural parameter ($\boldsymbol{\phi}_{av}$) reflects the degree of structural flexibility of the tetrahalidocuprate(II) moiety. With a series of known X-ray structures combined with EPR parameters of tetrabromidocuprates(II) it could be possible to classify the degree of distortion between square planar and tetrahedral geometries, as well as those of complexes with unknown structures as was recently shown for tetrabromidocuprates(II) [34]. With larger the *cis*-angles the g_{av} or the isotropic g_{iso}-values have a tendency to increase (see Figure 4). This is also supported by calculated values from DFT calculations.

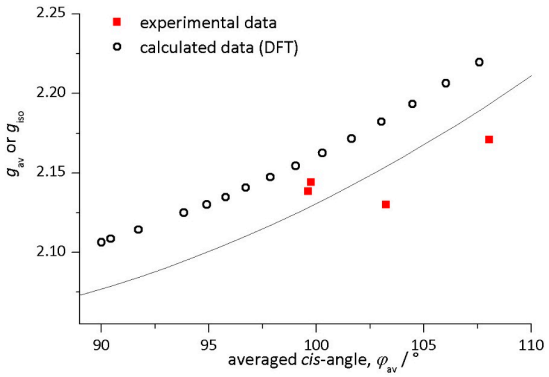

Figure 4. Correlation of EPR parameter (g_{av}/g_{iso}) with the coordination geometry (averaged *cis*-angle) including the four new data sets from Table 6 (squares); the circles represent the calculated data (DFT).

Figure 5 shows the temperature-dependent EPR spectra of $(EtPh_3P)_2[CuBr_4]$ (**7**) recorded in a temperature range from 300 to 430 K. The signal intensity decreases with rising temperature until it is fully distinct, due to spin saturation effects. This thermal cycle is completely reversible without any signs of decomposition. Interestingly, after cooling to room temperature, only an isotropic EPR signal remains (Figure 6), which returned to the starting axial symmetric spectrum after a couple of days (Figure 7). Obviously the re-crystallization process is kinetically enhanced. Compounds of this type might be useful as ionic liquids for higher temperatures.

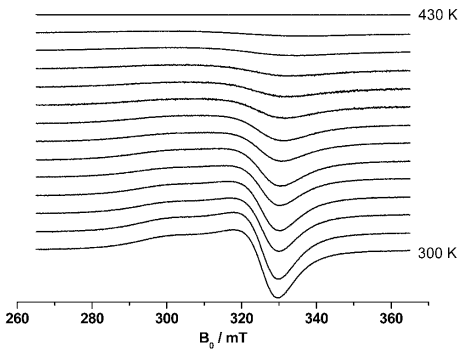

Figure 5. Temperature dependent EPR spectra of $(EtPh_3P)_2[CuBr_4]$ (**7**) recorded in the temperature range from 300 to 430 K (10 K steps).

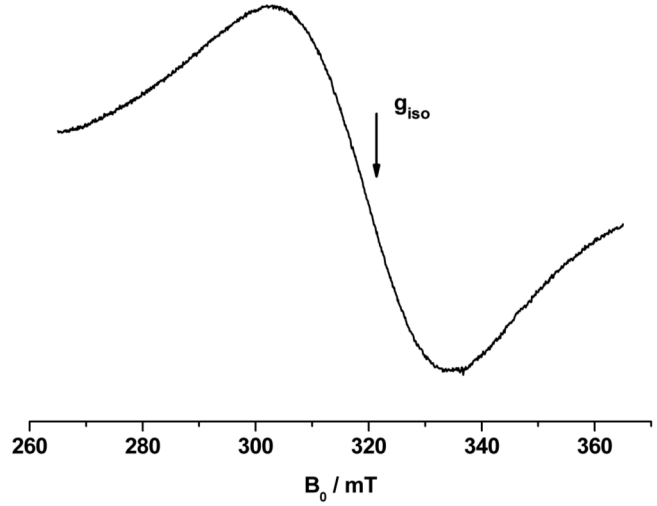

Figure 6. EPR spectrum of $(EtPh_3P)_2[CuBr_4]$ (**7**) at 150 K directly after the thermal treatment; only an isotropic signal remains.

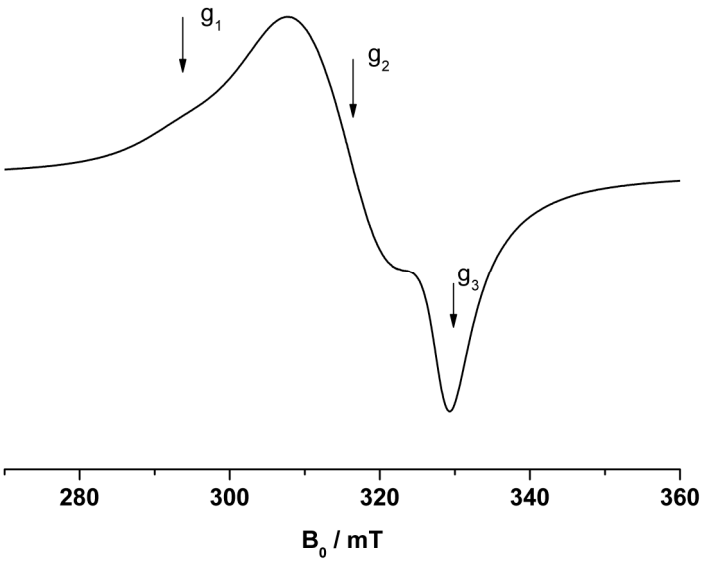

Figure 7. EPR spectrum of $(C_{12}H_{25}Me_3N)_2[CuBr_4]$ (**9**) at 110 K.

The EPR spectrum of $(C_{12}H_{25}Me_3N)_2[CuBr_4]$ (**9**) at 110 K (Figure 7) reflects a rhombic symmetry of the *g*-tensor with three different *g*-values and indicates a change in coordination geometry or a possible lamellar structure.

2.5. Differential Scanning Calorimetry (DSC)

$(EtPh_3P)_2[CuBr_4]$ (**7**) shows a glass transitions at 306 K, a melting point at 432 K and a cold crystallization by 369 K. Figure 8 shows the second heat run of the compound. The third measurement comes to the same result as the second. It can be concluded that the compound has a temperature reversibility at least up to 443 K. The results of the differential scanning calorimetry of (**7**) are in good agreement with the data from EPR-spectroscopy.

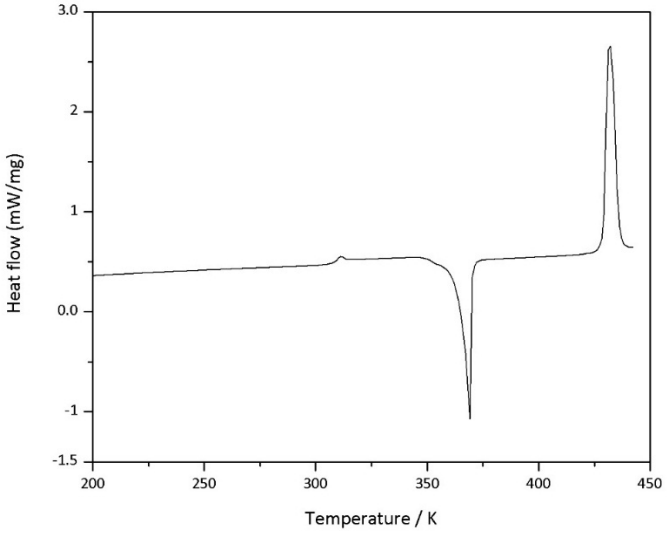

Figure 8. Second DSC scan from $(EtPh_3P)_2[CuBr_4]$ (**7**).

3. Materials and Methods

3.1. Methods

The melting points were determined using a Mikroheiztisch Boetius (VEB Wägetechnik, Radebeul, DDR). Elemental analyses were carried out on an Elementar Vario EL III analyzer (elementar Analysensysteme GmbH, Hanau, Germany). Infrared spectra were recorded on a Perkin-Elmer type 16PC FT-IR spectrophotometer (Perkin-Elmer GmbH, Überlingen, GErmany) between 4000 and 400 cm^{-1} as KBr-pellets (reference KBr). The measurements of the magnetic susceptibility were performed with a Magnetic Susceptibility Balance-Auto from Johnson Matthey GmbH (Matthey GmbH, Cambridge, UK) at room temperature, for diamagnetic correction the increment system of Pascal and Pacault [38] was applied. EPR spectra were recorded at 9.4 GHz (X-band) using a Bruker CW Elexsys E 500 spectrometer (Bruker BioSpin GmbH, Rheinstetten, Germany)

For X-ray structure determinations, the crystals were embedded in perfluoropolyalkylether oil and mounted on a glass fibre (**5**) or within a MicroGripper (**8**). For structure analysis of (**5**), the intensity data were collected at 210 K using an Imaging Plate Diffraction System IPDS-2 (Stoe, Darmstadt, Germany) with graphite monochromatized Mo-$K\alpha$ radiation (λ = 0.71073 Å) at 50 kV and 40 mA. The data collection for (**8**) was performed on a StadiVari diffractometer (Stoe, Darmstadt, Germany) equipped with a four-circle goniometer (open Eulerian cradle), a Genix Microfocus X-ray source (Mo) with a graded multilayer mirror and a Pilatus 200 K detector (Dectris, Baden-Daettwil, Switzerland). The data were corrected for absorption as well as for Lorentz polarization and extinction effects using the program X-Area (Stoe, 2004) [39]. The structures were solved by direct methods using SHELXS-2013/1 [40] and refined by full-matrix least squares on F^2 using the program SHELXL-2014/7 [41]. All non-hydrogen atoms were refined anisotropically. The hydrogen atoms were calculated in their expected positions and refined with a riding model. CCDC 1459578 (**5**) and CCDC 1459612 (**8**) contain the supplementary crystallographic data for this paper. These data are provided free of charge by The Cambridge Crystallographic Centre (Cambridge, UK).

Differential scanning calorimetry (DSC) measurements were performed with a DSC 214 Polyma (Netzsch GmbH & Co. KG, Selb, Germany) by NETZSCH operating with a scan rate of 5–10 °C· min^{-1} under a nitrogen flow.

3.2. Chemicals

The following chemicals were used without further purification. Copper(II) bromide (99%), ethanol anhydrous (99%), n-hexane (96%), potassium bromide (Uvasol, Merk KGaA, Darmstadt, Germany, for IR spectroscopy) tetraethylammonium bromide (98%), tetrabutylphosphonium bromide (99%), tetrahexylammonium bromide (99%), benzyltrimethylammonium bromide (98%), benzyltriethylammonium bromide (98%), benzyltributylammonium bromide (99%), ethyltriphenylphosphonium bromide (98%), hexyltriphenylphosphonium bromide (>99%), dodecyltrimethylammonium bromide (>98%), hexadecylpyridinium bromide (98%), and dihexadecyldimethylammonium bromide (99%).

3.3. Syntheses

3.3.1. General Preparation

In general, tetrabromidocuprate(II) complexes can be achieved by different procedures [42–44]. In the current work, the $[CuBr_4]^{2-}$ moiety was synthesized according to a protocol by N. S. Gill and R. S. Nyholm [44]: an ethanolic solution of a stoichiometric amount of $CuBr_2$ was added to the respective bromide salt of the cation dissolved in a minimum volume of ethanol. The reaction mixture was stirred for one hour at room temperature. The product was precipitated by evaporating the solvent.

3.3.2. Bis(tetraethylammonium)tetrabromidocuprate(II), $(Et_4N)_2[CuBr_4]$ (**1**)

Compound (**1**) was synthesized according to an already published protocol [36].

A solution of 1.5 mmol (0.32 g) of tetraethylammonium bromide in 3 mL of ethanol was mixed with a solution of 0.5 mmol (0.11 g) of copper(II) bromide in 10 mL ethanol. The solution was stirred one hour at room temperature. The solvent was removed and a violet powder was received, filtered off and dried.

Melting point: 241–242 °C. Yield: 0.22 g (67%). Elemental analysis calculated for $C_{16}H_{40}N_2CuBr_4$ (643.66): C 29.85, H 6.26, N 4.35 (%); found: C 29.80, H 6.20, N 4.34 (%). IR (KBr, cm^{-1}): 3443 s, 2976 m, 2921 m, 2852 wm, 1628 wm, 1478 s, 1402 m, 1307 w, 1183 m, 1032 m, 1006 m, 793 m.
(IR: s = strong, ms = medium strong, m = medium, wm = weak medium, w = weak).

3.3.3. Bis(tetrabutylphosphonium)tetrabromidocuprate(II), $(Bu_4P)_2[CuBr_4]$ (**2**)

Solutions of 0.5 mmol (0.11 g) copper(II) bromide and 1.0 mmol (0.32 g) tetrabutylphosphonium bromide, each dissolved in 2 mL ethanol, were combined and stirred at room temperature for 1 h. The resulting violet precipitate is filtered off and dried.

Melting point: 49–52 °C. Yield: 0.38 g (84%). Elemental analysis calculated for $C_{32}H_{72}P_2CuBr_4$ (902.13): C 42.60, H 8.04 (%), found: C 42.08, H 8.16 (%). IR (KBr, cm^{-1}): 2928 s, 2891 ms, 2870 ms, 1463 ms, 1407 m, 1375 m, 1237 w, 1098 m, 968 w, 920 m, 722 m. μ_{eff} = 1.5 B.M.

3.3.4. Bis(tetrahexylammonium)tetrabromidocuprate(II), $(Hex_4N)_2[CuBr_4]$ (**3**)

A solution of 1.0 mmol (0.22 g) $CuBr_2$ in 5 mL ethanol was added to a solution of 2.0 mmol (0.87 g) tetrahexylammonium bromide in 5 mL ethanol. The mixed solution was stirred at room temperature for 1 h. The resulting violet precipitate was filtered off and dried.

Melting point: 93–95 °C. Yield: 0.58 g (53%). Elemental analysis calculated for $C_{48}H_{104}N_2CuBr_4$ (1092.51): C 52.77, H 9.60, N 2.56 (%), found: C 53.06, H 9.70, N 2.67 (%). IR (KBr, cm^{-1}): 2928 s, 2553 m, 1634 w, 1480 m, 1383 mw, 1050 w, 728 w. μ_{eff} = 1.5 B.M.

3.3.5. Bis(benzyltrimethylammonium)tetrabromidocuprate(II), $(BzlMe_3N)_2[CuBr_4]$ (**4**)

Compound (**4**) was also synthesized according to an already published procedure [37].

To a solution of 0.5 mmol (0.11 g) of $CuBr_2$ in 3.5 mL methanol a solution of 1.0 mmol (0.23 g) benzyltrimethylammonium bromide, dissolved in 1.5 mL methanol, was added. The mixture was stirred for one hour at room temperature. After a short while the complex precipitated as purple crystals.

Melting point: 173–175 °C. Yield: 0.35 g (72%). Elemental analysis calculated for $C_{20}H_{32}N_2CuBr_4$ (969.51): C 35.16, H 4.72, N 4.10 (%); found: C 35.09, H 4.71, N 4.17 (%). IR (KBr, cm^{-1}): 3017 m, 1585 w, 1485 s, 1476 s, 1411 m, 1218 m, 989 m, 974 m, 887 s, 780 s, 703 s. μ_{eff} = 1.4 B.M.

3.3.6. Bis(benzyltriethylammonium)tetrabromidocuprate(II), $(BzlEt_3N)_2[CuBr_4]$ (**5**)

0.5 mmol (0.11 g) of $CuBr_2$ dissolved in 3 mL HBr was heated under reflux for 0.5 h. To this copper solution a solution of 1.0 mmol (0.27 g) $BzlEt_3NBr$ and 2 mL methanol was slowly added. The mixture was stirred for one hour at room temperature. The solvent was reduced and purple crystals were obtained by covering the remaining solution with *N*-hexane.

Melting point: 110–112 °C. Yield: 0.21 g (54%). Elemental analysis calculated for $C_{26}H_{44}N_2CuBr_4$ (767.7): C 40.67, H 5.78, N 3.65 (%); found: C 40.56, H 5.76, N 3.69 (%). IR (KBr, cm^{-1}): 2983 m, 1583 w, 1450 s, 1402 ms, 1372 w, 1171 w, 1154 m, 1027 m, 1005 m, 787 m,756 s, 705 s. μ_{eff} = 1.6 B.M.

3.3.7. Bis(benzyltributylammonium)tetrabromidocuprate(II), $(BzlBu_3N)_2[CuBr_4]$ (**6**)

A solution of 1.0 mmol (0.22 g) $CuBr_2$ in 5 mL ethanol was added to a solution of 2.0 mmol (0.71 g) benzyltributylammonium bromide in 5 mL ethanol. The mixed solution was stirred at room temperature for 1 h. The resulting violet precipitate was filtered off and dried.

Melting point: 58–60 °C. Yield: 0.59 g (63%). Elemental analysis calculated for $C_{38}H_{68}N_2CuBr_4$ (936.12): C 48.75, H 7.32, N 2.99 (%), found: C 48.90, H 7.48, N 3.12 (%). IR (KBr, cm^{-1}): 2959 s, 2871 m, 1654 w, 1561 w, 1474 m, 1458 m, 1380 mw, 1212 w, 869 mw, 725 m, 704 m. μ_{eff} = 1.5 B.M.

3.3.8. Bis(ethyltriphenylphosphonium)tetrabromidocuprate(II), $(EtPh_3P)_2[CuBr_4]$ (**7**)

The synthesis of $(EtPh_3P)_2[CuBr_4]$ as follows: 0.5 mmol (0.11 g) copper(II) bromide and 1.0 mmol (0.37 g) $EtPh_3PBr$ solved even in 2 mL ethanol. The combined solutions are stirred for one hour at room temperature. A violet powder was obtained.

Melting point: 135–137 °C. Yield: 0.23 g (48%). Elemental analysis calculated for $C_{40}H_{40}P_2CuBr_4$ (964.90): C 49.74, H 4.17 (%), found: C 49.74, H 4.19 (%). IR (KBr, cm^{-1}): 2922 m, 1586 m, 1483 m, 1438 s, 1113 s, 996 m, 780 w, 739 s, 691 s, 531 s, 510 s, 482 m. μ_{eff} = 1.6 B.M.

3.3.9. Bis(hexyltriphenylphosphonium)tetrabromidocuprate(II), $(HexPh_3P)_2[CuBr_4]$ (**8**)

A solution of 1.0 mmol (0.22 g) copper(II) bromide in 5 mL ethanol is added to 2.0 mmol (0.85 g) hexyltriphenylphosphonium bromide dissolved in 5 mL ethanol. The solution was stirred for 1 h at room temperature. The formed violet precipitate was filtered off and dried. Purple crystals were obtained by covering the remaining solution with n-hexane for slowly interdiffusion.

Melting point: 102–103 °C. Yield: 0.65 g (60%). Elemental analysis calculated for $C_{48}H_{56}P_2CuBr_4$ (1078.04): C 53.47, H 5.24 (%), found: C 53.05, H 4.97 (%). IR (KBr, cm^{-1}): 2956 m, 2923 m, 2758 m, 1585 w, 1485 w, 1436 s, 1113 s, 724 s, 689 s, 533s, 498 ms. μ_{eff} = 1.6 B.M.

3.3.10. Bis(dodecyltrimethylammonium)tetrabromidocuprate(II), $(C_{12}H_{25}Me_3N)_2[CuBr_4]$ (**9**)

A solution of 1.0 mmol (0.22 g) of $CuBr_2$ in 5 mL ethanol and a solution of 2.0 mmol (0.62 g) $C_{12}H_{25}Me_3NBr$ in 5 mL ethanol were combined and stirred at room temperature for 1 h. The resulting violet precipitate was filtered off and dried.

Melting point: 94–95 °C. Yield: 0.56 g (85%). Elemental analysis calculated for $C_{30}H_{48}N_2CuBr_4$ (662.23): C 42.89, H 8.16, N 3.34 (%), found: C 43.19, H 8.23, N 3.37 (%). IR (KBr, cm^{-1}): 2922 ms, 2851 m, 1632 w, 1469 s, 966 ms, 909 m, 722 m. μ_{eff} = 1.5 B.M.

3.3.11. Bis(hexadecylpyridinium)tetrabromidocuprate(II), $(C_{16}\text{-py})_2[CuBr_4]$ (**10**)

A solution of 0.5 mmol (0.11 g) copper(II) bromide in 10 mL ethanol is added to 1.0 mmol (0.40 g) hexadecylpyridinium bromide dissolved in 3 mL ethanol. The solution was stirred for 1 h at room temperature. The obtained violet precipitate was filtered off and dried.

Melting point: 73–74 °C. Yield: 0.15 g (30%). Elemental analysis calculated for $C_{42}H_{76}N_2CuBr_4$ (992.23): C 50.84, H 7.72, N 2.82 (%), found: C 47.67, H 7.20, N 2.95 (%). IR (KBr, cm^{-1}): 3446 wm, 3053 w, 2918 s, 2850 m, 1633 wm, 1485 m, 1468 wm, 1175 w, 768 w, 721 w, 679 w. μ_{eff} = 1.6 B.M.

3.3.12. Bis(dihexadecyldimethylammonium)tetrabromidocuprate(II), $(C_{16}H_{33})_2Me_2N)_2[CuBr_4]$ (**11**)

A solution of 1.0 mmol (0.58 g) dihexadecyldimethylammonium bromide in 3 mL ethanol was slowly added to a solution of 0.5 mmol (0.11 g) copper(II) bromide in 3 mL ethanol. The mixture was stirred at room temperature for 1 h. The formed violet precipitate was filtered off and dried.

Melting point: 36–38 °C. Yield: 0.67 g (98%). Elemental analysis calculated for $C_{68}H_{144}N_2CuBr_4$ (1373.05): C 59.48, H 10.57, N 2.04 (%), found: C 59.11, H 10.89, N 2.15 (%). IR (KBr, cm^{-1}): 2919 m, 2851 m, 1628 w, 1469 s, 1376 w, 1054 w, 990 w, 968 w, 878 w, 718 m.

4. Conclusions

Some of the compounds in this series are real ionic liquids—(**2**), (**3**), (**6**), (**10**) and (**11**)—with melting points below 100 °C, or very close to it—(**5**) and (**8**). All the reported compounds are thermally stable up to at least 430 K. This thermal cycle is completely reversible without any signs of decomposition. Interestingly, after cooling to room temperature, for (**7**) only an isotropic EPR signal remains, which returned to the axial symmetric spectrum after a couple of days. That means the re-crystallizing process is kinetically enhanced. Compounds of this type might be useful as ionic liquids for higher temperatures.

Two compounds, (**5**) and (**8**), could be structurally characterized by X-ray structure analysis. The structures are stabilized by a variety of hydrogen contacts between the $[CuBr_4]^{2-}$ anions and corresponding onium cations, responsible for the coordination geometry of the tetrahalidocuprates. The EPR parameters also reflect the degree of structural flexibility of the tetrahalidocuprate(II) moiety. With a series available data sets of known X-ray structures combined with EPR parameters of tetrabromidocuprates(II) it is possible to classify the degree of the distortion coordination sphere between square planar and tetrahedral geometries, as was recently shown for tetrabromidocuprates(II) [34].

Acknowledgments: We acknowledge Ulf Steinhoff and Ahed Abouserie for DSC measurements and Anne Nitschke for recording the IR-spectra.

Author Contributions: André Zabel, Peter Strauch: writing of manuscript, analytical interpretation, literature search; André Zabel, Alette Winter: syntheses; Peter Strauch, Alette Winter: EPR spectroscopy; Alexandra Kelling, Uwe Schilde: X-ray crystallography.

Conflicts of Interest: The authors declare no conflict of interest.

Abbreviations

DFT Discrete Fourier Transform
EPR Electron Paramagnetic Resonance
DSC Differential Scanning Calorimetry

References

1. Taubert, A. Heavy elements in ionic liquids. *Top. Curr. Chem.* **2009**, *290*, 127–159.
2. Taubert, A. CuCl Nanoplatelets from an ionic liquid-crystal precursor. *Angew. Chem. Int. Ed.* **2004**, *43*, 5380–5382. [CrossRef] [PubMed]
3. Saito, G. Electric conductivity and magnetic ionic liquids. In *Electrochemical Aspects of Ionic Liquids*, 2nd ed.; Ohno, H., Ed.; John Wiley & Sons, Inc.: New York, NY, USA, 2011; pp. 337–346.
4. Kalb, R. Use of Magnetic, Ionic Liquids as an Extraction Agent. PCT Int. Pat. WO 2009080648 A1, 2 July 2009.
5. Dengler, J.E.; Doroodian, A.; Rieger, B. Protic metal-containing ionic liquids as catalysts: Cooperative effects between anion and cation. *J. Organomet. Chem.* **2011**, *696*, 3831–3835. [CrossRef]
6. Bica, K.; Gaertner, P. Metal-containing ionic liquids as efficient catalysts for hydroxymethylation in water. *Eur. J. Org. Chem.* **2008**, 3453–3456. [CrossRef]
7. Bica, K.; Gaertner, P. An iron-containing ionic liquid as recyclable catalyst for aryl grignard cross-coupling of aryl halides. *Org. Lett.* **2006**, *8*, 733–735. [CrossRef] [PubMed]
8. Lin, I.J.B.; Vasam, C.S. Metal-containing ionic liquids and ionic liquid crystals based on imidazolium moiety. *J. Organomet. Chem.* **2005**, *690*, 3498–3512. [CrossRef]
9. Bowlas, C.J.; Bruce, D.W.; Seddon, K.R. Liquid-crystalline ionic liquids. *Chem. Commun.* **1996**, 1625–1626. [CrossRef]
10. Neve, F.; Francescangeli, O.; Crispini, A.; Charmant, J. $A_2[MX_4]$ Copper(II) pyridinium salts. From ionic liquids to layered solids to liquid crystals. *Chem. Mater.* **2001**, *13*, 2032–2041. [CrossRef]
11. Neve, F.; Francescangeli, O.; Crispini, A. Crystal architecture and mesophase structure of long-chain *N*-alkylpyridinium tetrachlorometallates. *Inorg. Chim. Acta* **2002**, *338*, 51–58. [CrossRef]
12. Neve, F.; Crispini, A. C–H···Br–M Interactions at Work: Tetrabromometalates of the bolaamphiphilic *N*,*N*′-dodecamethylenedipyridinium cation. *Cryst. Growth Des.* **2001**, *1*, 387–393. [CrossRef]
13. Neve, F.; Crispini, A. C-H···Br-M Interactions at work: Tetrabromometalates of the bolaamphiphilic *N*,*N*′-dodecamethylenedipyridinium cation. *Cryst. Growth Des.* **2001**, *1*, 519. [CrossRef]
14. Taubert, A.; Palivan, C.; Casse, O.; Gozzo, F.; Schmitt, B. Ionic liquid-crystal precursors (ILCPs) for CuCl platelets: The origin of the exothermic peak in the DSC curves. *J. Phys. Chem. C* **2007**, *111*, 4077–4082. [CrossRef]
15. Taubert, A.; Steiner, P.; Mantion, A. Ionic liquid crystal precursors for inorganic particles: Phase diagram and thermal properties of a CuCl nanoplatelet precursor. *J. Phys. Chem. B* **2005**, *109*, 15542–15547. [CrossRef] [PubMed]
16. Willett, R.D.; Haugen, J.A.; Lebsack, J.; Morrey, J. Thermochromism in copper(II) chlorides. Coordination geometry changes in $CuCl_4^{2-}$ anions. *Inorg. Chem.* **1974**, *13*, 2510–2513. [CrossRef]
17. Thiel, K.; Klamroth, T.; Strauch, P.; Taubert, A. On the interaction of ascorbic acid and the tetrachloridocuprate ion $[CuCl_4]^{2-}$ in CuCl nanoplatelet formation from an ionic liquid precursor (ILP). *Phys. Chem. Chem. Phys.* **2011**, *13*, 13537–13543. [CrossRef] [PubMed]
18. Zhuravlev, O.E.; Verolainen, N.V.; Voronchikhina, L.I. Thermal stability of 1,3-disubstituted imidazolium tetrachloroferrates, magnetic ionic liquids. *Russ. J. Appl. Chem.* **2011**, *84*, 1158–1164. [CrossRef]
19. Branco, A.; Branco, L.C.; Pina, F. Electrochromic and magnetic ionic liquids. *Chem. Commun.* **2011**, *47*, 2300–2302. [CrossRef] [PubMed]

20. Neve, F.; Crispini, A.; Armentano, S. Synthesis, structure, and thermotropic mesomorphism of layered *N*-alkylpyridinium tetrahalopalladate(II) salts. *Chem. Mater.* **1998**, *10*, 1904–1913. [CrossRef]
21. Neve, F.; Francescangeli, O. Layered ω-substituted alkylpyridinium salts with inorganic anions: Effects of H-bonding patterns on the layer thickness. *Cryst. Growth Des.* **2005**, *5*, 163–166. [CrossRef]
22. Neve, F.; Crispini, A. Competitive interactions in carboxy-functionalized pyridinium salts: Crossover from O–H···O to O–H···X–M contacts. *Cryst. Eng. Commun.* **2007**, *9*, 698–703. [CrossRef]
23. Neve, F.; Crispini, A. *N,N′*-Dodecamethylene-bis(pyridinium) goes lamellar. Role of C–H···I, C–H···M, and I···I interactions in the crystal structure of its hexaiododipalladate(II) derivative. *Cryst. Eng. Commun.* **2003**, *5*, 265–268. [CrossRef]
24. Neve, F.; Crispini, A.; Francescangeli, O. Structural studies on layered alkylpyridinium iodopalladate networks. *Inorg. Chem.* **2000**, *39*, 1187–1194. [CrossRef] [PubMed]
25. Binnemans, K. Ionic liquid crystals. *Chem. Rev.* **2005**, *105*, 4148–4204. [CrossRef] [PubMed]
26. Goossens, K.; Lava, K.; Nockemann, P.; van Hecke, K.; van Meervelt, L.; Driesen, K.; Görller-Walrand, C.; Binnemans, K.; Cardinaels, C. Pyrrolidinium ionic liquid crystals. *Chem. Eur. J.* **2009**, *15*, 656–674. [CrossRef] [PubMed]
27. Suisse, J.-M.; Douce, L.; Bellemin-Laponnaz, S.; Maisse-Francois, A.; Welter, R.; Miyake, Y.; Shimizu, Y. Liquid crystal imidazolium salts: Towards materials for catalysis and molecular electronics. *Eur. J. Inorg. Chem.* **2007**, *2007*, 3899–3905. [CrossRef]
28. Dobbs, W.; Suisse, J.-M.; Douce, L.; Welter, R. Electrodeposition of silver particles and gold nanoparticles from ionic liquid-crystal precursors. *Angew. Chem. Int. Ed.* **2006**, *45*, 4179–4182. [CrossRef] [PubMed]
29. Lee, C.K.; Peng, H.H.; Lin, I.J.B. Liquid crystals of *N,N′*-dialkylimidazolium salts comprising palladium(II) and copper(II) ions. *Chem. Mater.* **2004**, *16*, 530–536. [CrossRef]
30. Herber, R.H.; Nowik, I.; Kostner, M.E.; Kahlenberg, V.; Kreutz, C.; Laus, G.; Schottenberger, H. Mössbauer spectroscopy and X-ray diffraction study of ^{57}Fe-labeled tetrachloroferrate(III)-based magnetic ionic liquids. *Int. J. Mol. Sci.* **2011**, *12*, 6397–6406. [CrossRef] [PubMed]
31. De Pedro, I.; Rojas, D.P.; Albo, J.; Luis, P.; Irabien, A.; Blanco, J.A.; Fernandez, J.R. Long-range magnetic ordering in magnetic ionic liquid: Emim[$FeCl_4$]. *J. Phys. Condens. Matter* **2010**, *22*, 296006. [CrossRef] [PubMed]
32. Sasaki, T.; Zhong, C.; Tada, M.; Iwasawa, Y. Immobilized metal ion-containing ionic liquids: Preparation, structure and catalytic performance in Kharasch addition reaction. *Chem. Commun.* **2005**, 2506–2508. [CrossRef] [PubMed]
33. Winter, A.; Zabel, A.; Strauch, P. Tetrachloridocuprates(II)-synthesis and electron paramagnetic resonance (EPR) spectroscopy. *Int. J. Mol. Sci.* **2012**, *13*, 1612–1619. [CrossRef] [PubMed]
34. Farra, R.; Thiel, K.; Winter, A.; Klamroth, T.; Pöppl, A.; Kelling, A.; Schilde, U.; Taubert, A.; Strauch, P. Tetrahalidocuprates(II)—Structure and EPR spectroscopy. Part 1: Tetrabromidocuprates(II). *New J. Chem.* **2011**, *35*, 2793–2803. [CrossRef]
35. Winter, A.; Thiel, K.; Zabel, A.; Klamroth, T.; Pöppl, A.; Kelling, A.; Schilde, U.; Taubert, A.; Strauch, P. Tetrahalidocuprates(II)—Structure and EPR spectroscopy. Part 2: Tetrachloridocuprates(II). *New J. Chem.* **2014**, *38*, 1019–1030. [CrossRef]
36. Starova, G.L.; Skripkin, M.Y.; Gusev, I.M. Structure of complex bromides crystallizing in MBr_2—NEt_4Br—H_2O systems (M = Cd, Cu, Co) at 25 °C. *Russ. J. Gen. Chem.* **2010**, *80*, 1236–1241. [CrossRef]
37. Jin, L.; Liu, N.; Li, Y.-J.; Wu, D.-H. Bis(benzyltrimethylammonium)tetrabromidocuprates(II). *Acta Crystallogr. Sect. E* **2011**, *E67*, m1325. [CrossRef] [PubMed]
38. Hellwege, K.-H.; Hellwege, A.M.; (Eds.) *Magnetic Properties of Coordination and Organo-Metallic Transition Metal Compounds. Landolt-BöRnstein—Group II, Atomic and Molecular Radicals*; Springer: New York, NY, USA, 1966; Volume 2.
39. *X-Area Vers. 1.26*. Stoe & Cie: Darmstadt, Germany, 2004.
40. Sheldrick, G.M. *SHELXS-2013/1, Program for the Crystal Structure Solution*; University Göttingen: Göttingen, Germany, 2013.
41. Sheldrick, G.M. *SHELXL-2014/7, Program for the Refinement of Crystal Structures*; University Göttingen: Göttingen, Germany, 2014.
42. Furlani, C.; Morpurgo, G. Properties and electron structure of tetrahalogenocuprate (II)-complexes. *Theor. Chim. Acta* **1963**, *1*, 102–115. [CrossRef]

43. Liu, H.; Wang, X.; Hu, W.; Guo, L.; Ouyang, S. Preparation and characterization of $(C_4H_9NH_3)_2CuX_4$ (X = Cl, Br). *Chem. J. Intern.* **2004**, *6*, 066039ne.
44. Gill, N.S.; Nyholm, R.S. Complex halides of the transition metals. Part I tetrahedral nickel complexes. *J. Chem. Soc.* **1959**, 3997–4007. [CrossRef]